Characterizing Congo Basin Rainfall and Climate Using Tropical Rainfall Measuring Mission (TRMM) Satellite Data and Limited Rain Gauge Ground Observations

YOLANDE A. MUNZIMI AND MATTHEW C. HANSEN

Department of Geographical Sciences, University of Maryland, College Park, College Park, Maryland

BERNARD ADUSEI

Radius Technology Group, Inc., Silver Spring, Maryland

GABRIEL B. SENAY

U.S. Geological Survey Earth Resources Observation and Science Center, Sioux Falls, South Dakota

(Manuscript received 31 December 2013, in final form 10 November 2014)

ABSTRACT

Quantitative understanding of Congo River basin hydrological behavior is poor because of the basin's limited hydrometeorological observation network. In cases such as the Congo basin where ground data are scarce, satellite-based estimates of rainfall, such as those from the joint NASA/JAXA Tropical Rainfall Measuring Mission (TRMM), can be used to quantify rainfall patterns. This study tests and reports the use of limited rainfall gauge data within the Democratic Republic of Congo (DRC) to recalibrate a TRMM science product (TRMM 3B42, version 6) in characterizing precipitation and climate in the Congo basin. Rainfall estimates from TRMM 3B42, version 6, are compared and adjusted using ground precipitation data from 12 DRC meteorological stations from 1998 to 2007. Adjustment is achieved on a monthly scale by using a regression-tree algorithm. The output is a new, basin-specific estimate of monthly and annual rainfall and climate types across the Congo basin. This new product and the latest version-7 TRMM 3B43 science product are validated by using an independent long-term dataset of historical isohyets. Standard errors of the estimate, root-mean-square errors, and regression coefficients r were slightly and uniformly better with the recalibration from this study when compared with the 3B43 product (mean monthly standard errors of 31 and 40 mm of precipitation and mean r^2 of 0.85 and 0.82, respectively), but the 3B43 product was slightly better in terms of bias estimation (1.02 and 1.00). Despite reasonable doubts that have been expressed in studies of other tropical regions, within the Congo basin the TRMM science product (3B43) performed in a manner that is comparable to the performance of the recalibrated product that is described in this study.

1. Introduction

Rainfall plays many important roles in the Earth system, including being the primary source of freshwater, defining conditions for diverse ecosystems, and enabling economic activities such as agriculture. As such, rainfall information from any given hydrological system is of crucial importance. To monitor rainfall over an area, timely information on precipitation dynamics is measured and distributed by meteorological station networks. Many of these networks are poorly distributed across the globe in general and across Africa in particular. As a result, rainfall regimes in Africa have not been sufficiently quantified because of a lack of ground rainfall data. A few authors, such as Nicholson (2000), have used historical ground-station information to characterize rainfall regimes and seasons at the continental scale. With station data being sparse, not covering concurrent time periods, and having incomplete time series, achieving consistency is a challenge. Speaking particularly about Africa, Dinku et al. (2007) wrote, "The number of rain gauges throughout Africa is small and unevenly distributed, and the gauge network is deteriorating. Satellite rainfall estimates are being used widely in place of gauge observations or to supplement gauge observations." The lack

Corresponding author address: Matthew C. Hansen, Dept. of Geographical Sciences, University of Maryland, College Park, 2181 Samuel J. LeFrak Hall, College Park, MD 20742.
E-mail: mhansen@umd.edu

DOI: 10.1175/JAMC-D-14-0052.1

of ground observations has led to the necessity of exploring alternative solutions such as satellite rainfall estimates to replace or augment ground data.

The extensive data records of gridded, satellite-based rainfall estimates at a variety of spatial resolutions provide improved means for the continental-scale mapping of rainfall regimes (Herrmann and Mohr 2011). This fact has motivated recent advances in rainfall characterization with satellite precipitation products. Rainfall classifications such as those by Dinku et al. (2007, 2008, 2010) or Herrmann and Mohr (2011) offer improved rainfall products for Africa. They have higher spatial resolutions than ground-based products do and are generated from data with temporal continuity.

The Congo basin in central Africa is one of the river systems for which ground-data availability is a limiting factor to rainfall-regime characterization. In such cases, satellite-based estimates of rainfall can be used to quantify rainfall patterns. Data from the joint NASA/JAXA Tropical Rainfall Measuring Mission (TRMM), which has been operational since January of 1998, are one such example. Throughout the last decade, validation studies performed using TRMM precipitation data within Africa present a reasonable level of accuracy (Adeyewa and Nakamura 2003; Nicholson et al. 2003; Dinku et al. 2007, 2010; Roca et al. 2010). These studies of TRMM products also suggest a slight underestimation of monthly-mean rainfall and increased uncertainties for some areas, however. TRMM science products such as the monthly TRMM 3B43, version 7, dataset (Huffman and Bolvin 2014) have been found to have limited accuracy even though they are calibrated using rain gauge data from the Global Precipitation Climatology Centre (GPCC) (Rudolf 1993; Rudolf et al. 1994; Huffman et al. 1997)—to be specific, the version-6 full GPCC data reanalysis (Huffman and Bolvin 2014). A reason adduced for this inaccuracy is the sparseness of GPCC gauge locations. The Congo basin is one such region that lacks GPCC gauge locations for the period of study (from 1998 to 2007). This lack is because of their absence in the Democratic Republic of Congo (DRC), which covers 60% of the Congo basin watershed. Because most of the GPCC gauges are concentrated in more-seasonal regions that are adjacent to the Congo basin, there is reason to believe that algorithms developed to calibrate TRMM science products in Africa likely favor the arid influence of these stations. As such, it is worth investigating the performance of TRMM 3B43 products over the Congo.

With regard to deficiencies in current gauge-calibrated analyses of Africa, Huffman et al. (2010) reported that it will continue to be the case that some underdeveloped areas, such as central Africa, will have greater uncertainty because of a lack of gauge inputs. Bitew and Gebremichael (2011) demonstrated that gauge-calibrated products likely have low accuracy for regions that lack rain gauge data. After comparing integrated satellite–gauge rainfall products with satellite-only products for the Nile basin, they suggested that users forego the conventional notion that satellite rainfall products that incorporate GPCC rain gauge data have higher accuracies than satellite-only products (Bitew and Gebremichael 2011). The mentioned limitation has also been attributed to the deficiency in gauge observations. A limited number of gauges in sparse regions have been reported to be unsuitable for Huffman et al's (1997) merging analysis for TRMM science products. Given these findings, alternative methods for gauge-sparse regions are warranted.

The purpose of this study is to test a calibration that uses limited/sparse in situ gauge data for Congo basin precipitation characterization. A generic feature space, or set of independent variables, is used to extrapolate the limited gauge data to the basin scale using version-6 TRMM 3B42 inputs and a regression-tree algorithm.

We recalibrate version-6 TRMM 3B42 satellite-derived rainfall data for the Congo basin using concurrent ground data from rain gauges located in the DRC. The 3B42 daily rainfall data are derived from 3-hourly observations as part of the TRMM Multisatellite Precipitation Analysis. These data consist of merged microwave, infrared, and spaceborne radar inputs and incorporate gauge data where feasible from the GPCC and from the Climate Assessment and Monitoring System [more details on the gauge analysis are in Huffman et al. (2007)]. In the absence of basinwide rainfall data concurrent to version-6 TRMM 3B42 to evaluate the output, we compare the recalibrated TRMM rainfall data with "WorldClim" isohyets derived from longer-term historical records (Hijmans et al. 2005). We also include a comparison of our modeled monthly precipitation estimates and WorldClim data with the latest TRMM gauge-calibrated standard monthly product, the version-7 TRMM 3B43 dataset.

In a region where the climate is principally driven by precipitation, accurate rainfall data are required to characterize regional climates. We therefore propose a classification of the Congo basin climate using our recalibrated TRMM data and temperature grids and compare it with climates that were derived using the version-7 TRMM 3B43 data and the version-6 TRMM 3B42 data. We also discuss seasonal rainfall patterns across the basin and relate monthly rainfall estimates to stream gauge data. Our goal is to assess standard and regionally calibrated TRMM products for future basin-scale hydrological modeling of the Congo that will employ the improved rainfall data in characterizing basin

streamflows. A climate classification will be used as the basis for grouping rivers and streams by climate type within the Congo basin to facilitate comparisons of runoff characteristics.

2. Data

a. Precipitation data

1) TRMM PRECIPITATION DATA AND DATA LIMITATIONS FOR THE CONGO PRECIPITATION SYSTEM

We wanted to select the most accurate and most uniformly processed TRMM precipitation products for the time frame coincident with available recent in situ gauge data (1998–2007). When comparing versions 6 and 7 of the TRMM Multisatellite Precipitation Analysis (Huffman et al. 2010) precipitation products, TRMM data producers Huffman and Bolvin (2014) reported that product series for version 7 were retrospectively processed back to 2000 and not before. More relevant to our purpose is the need to maximize the record's length coincident with available gauge data for the DRC. Version 6 of the TRMM science product 3B42 (Huffman 2013) was consistently produced from 1998 to 2007. We consider the extra years to be valuable for model calibration and chose to employ version 6 of the TRMM 3B42 product as our model inputs. These inputs are employed to estimate precipitation at a 3-h temporal resolution and a 0.25° × 0.25° spatial resolution in a global belt extending from 50°S to 50°N latitude. Daily accumulations of the data are processed and hosted at the U.S. Geological Survey (USGS) Earth Resources Observation and Science (EROS) Center. The 0.25° version-6 TRMM 3B42 product has complete spatial coverage for Africa. The daily grids from 1998 to 2007 were summed to a monthly interval. These monthly aggregate 3B42 data (hereinafter, TRMM 3B42) are used as inputs for recalibration by monthly local gauge data and are made comparable to the TRMM 3B43 monthly product. For the purposes of comparison, we chose to use the most recent version of the GPCC gauge-calibrated TRMM 3B43 standard science product (version 7).

Limitations of TRMM real-time products and science products have been documented in detail and include underestimation of convective and stratiform rain regimes. Huffman et al. (2007) quantified gaps in 3-h combined microwave precipitation estimates that can omit convective precipitation events in the version-6 TRMM 3B42 product. There is also a lack of sensitivity to light precipitation that results in regionally dependent underestimations of rainfall in the TRMM 3B42 archive (Huffman and Bolvin 2014). Comparing estimates from heavy, convective, warm-season regimes and light, stratiform, cool-season regimes, Ebert et al. (2007) found convective rain better quantified by TRMM real-time data. Such TRMM product limitations have implications for rainfall regime estimation in the Congo.

Because of the Congo basin's location straddling the equator, convective and convergence systems are predominant. They are controlled by the northward and southward movement of the intertropical convergence zone and by the eastward and westward movement of the Congo air boundary (Tierney et al. 2011). Convective systems are fast moving, are of small extent and short duration, and are characterized by thunderstorms and squall lines. Stratiform or frontal rainfall generated by convergence systems is usually slow moving, of large extent, and of low intensity. For the entire tropics, however, Houze (1997) has suggested that, even though most precipitation in the tropics appears to be convective, the tropics show large radar echoes composed of convective rain alongside stratiform precipitation, with the stratiform echoes covering large areas and accounting for a large portion of tropical rainfall. Even if a significant portion of tropical rainfall is stratiform, however, Schumacher and Houze (2003) cited central Africa as one of the areas where convective rain amounts are high and stratiform rain fractions are low (20%–30%).

2) GROUND PRECIPITATION DATA

For this study, data on precipitation regime were obtained from 12 meteorological stations that are within the DRC and are managed by the DRC meteorological agency, Agence Nationale de Météorologie et de Télédétection par Satellite (METTELSAT). The ground precipitation data reported in this nationally held dataset are concurrent with TRMM observations. The limited number of operational stations represents a sparse and unevenly distributed rainfall gauge network within the DRC. Concerns of nonrepresentativeness of the station sample can be legitimately raised, but it has been demonstrated that the general spatiotemporal variation of rainfall over Africa can be described by using time series from a few selected regions (Nicholson 2000). Although such an approach has limitations over large areas, it is posited here that the different rainfall regimes of the Congo basin can be described with the available ground measurements. In addition, the proposed method generalizes the relationship between the ground data and TRMM 3B42 inputs using a geographic and time-insensitive feature space (see section 3). Figure 1 shows the extent of the Congo basin and the locations of available time series precipitation data from ground gauge measurements versus GPCC gridded precipitation gauge stations locations for 2005.

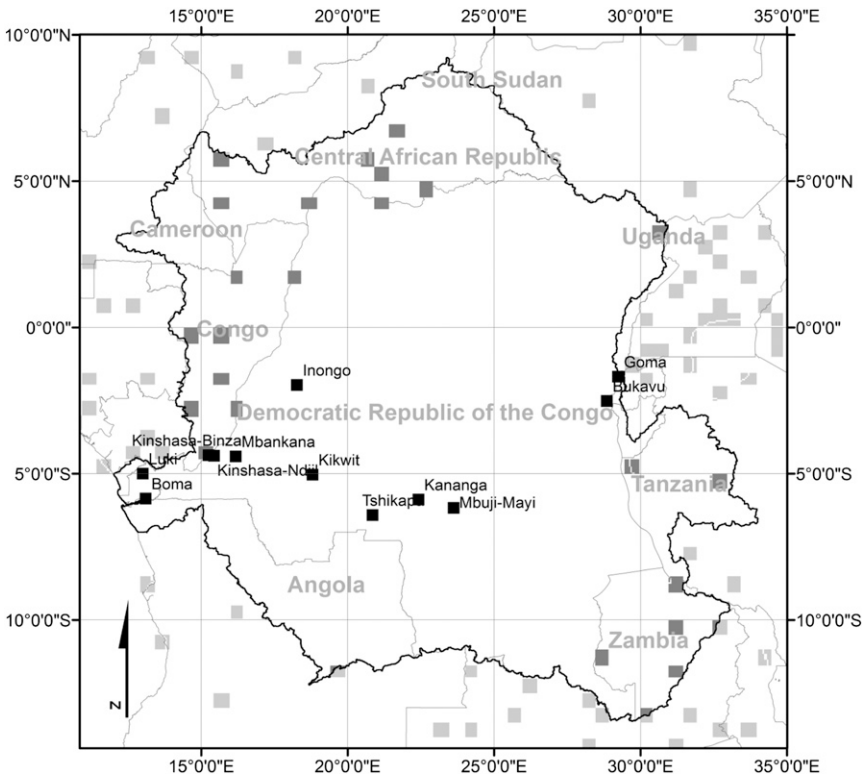

FIG. 1. The Congo basin with GPCC gridded precipitation gauge stations locations (dark-gray squares for the ones in the basin, and light-gray squares for those outside the basin) for 2003, available through the ''Visualizer'' (http://kunden.dwd.de/GPCC/Visualizer). The black squares are the the 12 precipitation gauge stations used in this study.

3) WORLDCLIM CLIMATOLOGICAL PRECIPITATION DATA

The independent validation dataset used for this study is the WorldClim precipitation model of Hijmans et al. (2005). WorldClim data are used to validate the monthly-mean recalibrated TRMM product averaged over the 10 years of study (1998–2007). WorldClim interpolated grids have been developed for global land areas at a spatial resolution of 30 arc s (1 km). In the Hijmans et al. study, WorldClim monthly-mean rainfall was averaged over 10 years for the Congo region, with most of the records preceding 1960 for the DRC. Hijmans et al. (2005) aggregated WorldClim monthly-mean precipitation data from historical records collected during the colonial period in the Congo region, meaning WorldClim monthly-mean data are not concurrent to the timeframe of our study (1998–2007). Despite the difference between the time periods of the datasets, the basinwide coverage of WorldClim affords a valuable basis for intercomparison, if one assumes that there has been no significant recent climate change within the region.

In the absence of ground information concurrent to TRMM, long-term averaged observed rainfall data have been used extensively to perform climatological validation of TRMM products [in West Africa by Nicholson et al. (2003), in Cyprus by Gabella et al. (2006, 2008), and many others]. In addition, a long-term record of 45 years (1960–2005) available for one station of the Congo basin at Kinshasa (Fig. 2) shows a relatively steady and even slightly upward trend of the annual rainfall over these years. Zhou et al. (2014) quantified a more recent decline in basinwide precipitation for selected months. Our decadal-scale approach should be less sensitive to such variations, but reservations could be raised about the comparison of dated WorldClim data and more recent TRMM precipitation estimates.

b. *Temperature data*

WorldClim mean temperature grids are used in combination with TRMM 3B42, recalibrated TRMM, and TRMM 3B43 data to map new climate classifications for the Congo basin with respect to rules from the Köppen–Geiger climate-classification system (Köppen 1884, 1918; Kottek et al. 2006; Peel et al. 2007). The climate in the Congo is principally driven by rainfall, with slight influences of temperature. There are no thermal seasons,

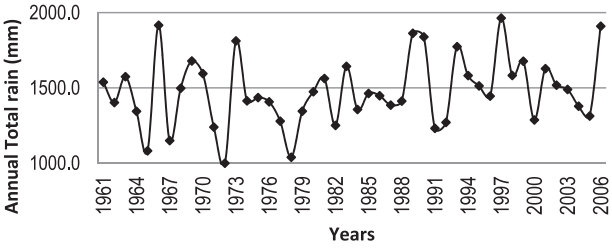

FIG. 2. Annual total precipitation (mm) at Kinshasa/N'djili station (1961–2006).

with the temperature representing a uniform picture and low annual range. The high altitudes of the eastern and southern fringes of the basin have the highest annual temperature range of 4°.

c. Climate data

Updated Köppen–Geiger climate data (Peel et al. 2007) were used for spatial comparison with TRMM-derived climate-classification products in the Congo. The updated Köppen–Geiger (K–G) dataset has a spatial resolution of 0.1° latitude/longitude. The climate system characterized by Peel et al. (2007) is based on global annual and monthly averages of interpolated temperature and precipitation data. Climate variables (temperature and precipitation) used in the K–G system were calculated at each station and interpolated between stations using a two-dimensional (latitude and longitude) thin-plate spline onto a 0.1° × 0.1° grid for each continent [more details on the analysis are in Peel et al. (2007)].

3. Methods

a. Rainfall estimation

A regression-tree algorithm was used to relate TRMM 3B42 data to gauge data. Regression trees are distribution-free models that reduce the overall sum of squares for a continuous dependent variable, in this case precipitation, by recursively partitioning the dataset into less-varying subsets, referred to as nodes (Breiman et al. 1984). For ease and speed of implementation, we employed a bagging method to avoid overfitting of the model (Breiman 1996). The first step consisted of preparing 25 samples, each consisting of 10% of the population of 10 years (1998–2007) of monthly rainfall observed at the 12 gauges. The sampled datasets were used to build 25 regression trees, and the median of the 25 model results was taken as the final estimate. The tree models predicted the sampled population of monthly rainfall data observed at the 12 gauges using nine independent variables (statistics) generated from daily TRMM 3B42 observations. The variables included TRMM 3B42 monthly total, TRMM 3B42 monthly average, minimum, 10th percentile, 25th percentile, 50th percentile, 75th percentile, 90th percentile, and maximum rainfall. All input variables were created without regard to specific month or specific region, enabling the creation of a generic feature space for basinwide extrapolation. After model application, each grid cell over the Congo basin was assigned a series of recalibrated monthly precipitation values from 1998 to 2007. These 10 years of recalibrated TRMM monthly total were then averaged to generate a rainfall climatological dataset or monthly rainfall records.

b. Climatological validation of recalibrated TRMM data

WorldClim climatological historical isohyet ranges (Hijmans et al. 2005) were compared with recalibrated monthly and annual precipitation data to validate model outputs. The long-term isohyet data were derived from a rich, if dated, historical record. The standard error of the predicted value (STEYX) for each x in the regression, the mean bias error (MBE), the root-mean-square error (RMSE), and coefficients of determination r^2 were used to measure the correspondence of the TRMM 3B42, TRMM 3B43, and recalibrated TRMM data to the historical precipitation record. The comparison was made for the 30 072 grid cells that constitute the Congo basin. In addition, biases that express systematic differences were calculated for every month.

The expression for the STEYX used for evaluation is

$$\mathrm{STEYX} = \left(\frac{1}{(N-2)}\left\{\sum(y-\bar{y})^2 - \frac{\left[\sum(x-\bar{x})(y-\bar{y})\right]^2}{\sum(x-\bar{x})^2}\right\}\right)^{1/2},$$

where x = WorldClim rainfall values, y = satellite rainfall predicted value, $\bar{x}$ and $\bar{y}$ = their corresponding means, and N = number of data pairs. Mean bias error and root-mean-square error were calculated respectively as

$$\mathrm{MBE} = \left[\sum(S-G)\right]/N \quad \text{and}$$

$$\mathrm{RMSE} = \left\{\left[\sum(S-G)^2\right]/N\right\}^{1/2},$$

TABLE 1. Key description of Köppen climate symbols and defining criteria, as adapted from Kottek et al. (2006) and Peel et al. (2007) for the central African region. Tann is the annual-mean near-surface (2 m) temperature (°C), and Tmax and Tmin are the monthly-mean temperatures of the warmest and coldest months, respectively. Pann is the accumulated annual precipitation, and Pmin is the precipitation of the driest month. Psmin, Psmax, Pwmin, and Pwmax are defined as the lowest and highest monthly precipitation values for the summer and winter half years on the hemisphere considered. All temperatures are in degrees Celsius, monthly precipitations are in millimeters per month, and Pann is in millimeters per year. In addition to these temperature and precipitation values, a dryness threshold Pth (mm) is introduced for the arid climates (B) that depends on Tann and the annual cycle of precipitation. Pth varies according to the following rules: if 70% of Pann occurs in winter then Pth = 2 × Tann, if 70% of Pann occurs in summer then Pth = 2 × Tann + 28, and otherwise Pth = 2 × Tann + 14. Summer (winter) is defined as the warmer (cooler) 6-month period of October–March and April–September. Tmon denotes the mean monthly temperature (°C). When needed, a third letter (column labeled "2nd") is included to indicate temperature.

Type			
1st	2nd	Description	Criterion
A		Equatorial climates	Tmin ≥ +18°C
Af		Equatorial rain forest, fully humid	Pmin ≥ 60 mm
Am		Equatorial monsoon	Not Af and Pann ≥ 25(100 − Pmin)
Aw		Equatorial savannah with dry winter	Not Af and Pmin < 60 mm in winter
B		Arid climates	Pann < 10 Pth
BS		Steppe climate	Pann > 5 Pth
BW		Desert climate	Pann ≤ 5 Pth
	h	Hot steppe/desert	Tann ≥ +18°C
	k	Cold steppe/desert	Tann < +18°C
C		Warm temperate climates	−3° < Tmin < +18°C
Cs		Warm temperate climates with dry summer	Psmin < Pwmin; Pwmax > 3 Psmin; Psmin < 40
Cw		Warm temperate climates with dry winter	Pwmin < Psmin and Psmax > 10 Pwmin
Cf		Warm temperate climates, fully humid	Neither Cs nor Cw
	a	Hot summer	Tmax ≥ +22°C
	b	Warm summer	Not "a" and at least 4 Tmon ≥ +10°C
	c	Cold summer	Not "b" and Tmin > −38°C
H		Highland climate	Tmax < +10°C

where G = gauge rainfall measurement, S = satellite rainfall estimate, and N = number of data pairs. MBE and RMSE are measured in millimeters. The expression for the bias statistic used for evaluation is

$$\text{bias} = \sum C / \sum I,$$

where I = interpolated rainfall grid and C = satellite rainfall estimate. Bias is dimensionless. Note that precalibration, r^2, MBE, and RMSE were also used to evaluate the performance of TRMM 3B42 satellite products in estimating the amount of the rainfall on the basis of comparison at gauges with observed data concurrent to TRMM 3B42.

c. *Rainfall- and temperature-based climate characterization*

From the precipitation products and the WorldClim temperature products, spatially explicit climate maps for the Congo basin were created by following the Köppen climate-classification rules shown in Table 1 (Köppen 1884, 1918; Kottek et al. 2006; Peel et al. 2007). Precipitation products were averaged to mean monthly rainfall over the period of observation (10 years for TRMM 3B42, TRMM 3B43, and recalibrated TRMM precipitation data). A similar averaging procedure was performed by Hijmans et al. (2005) for the WorldClim temperature grids.

A climate system characterized by Peel et al. (2007) that is based on the annual and monthly averages of interpolated temperature and precipitation data was compared with the new climate classifications, in which the interpolated precipitation data were replaced by TRMM 3B42, TRMM 3B43, and recalibrated TRMM-derived precipitation. These three maps were compared with the map of Peel et al. (2007) to quantify climate-type extent and overall agreement. Quantitative agreement was assessed by comparing the reference dataset (Peel's map) with the recalibrated TRMM-derived classified images. A confusion matrix—a common image-classification accuracy-assessment technique including overall, producer's, and user's accuracy—was employed. In the absence of a regional classification for the Congo region, the Peel et al. (2007) K–G climate classification is used in this study as the default reference.

4. Results

a. *Comparison of ground rain gauge and TRMM 3B42 data*

TRMM precipitation data from the version-6 3B42 product used in this study were compared with within-region rain gauge data. Monthly precipitation data for 4

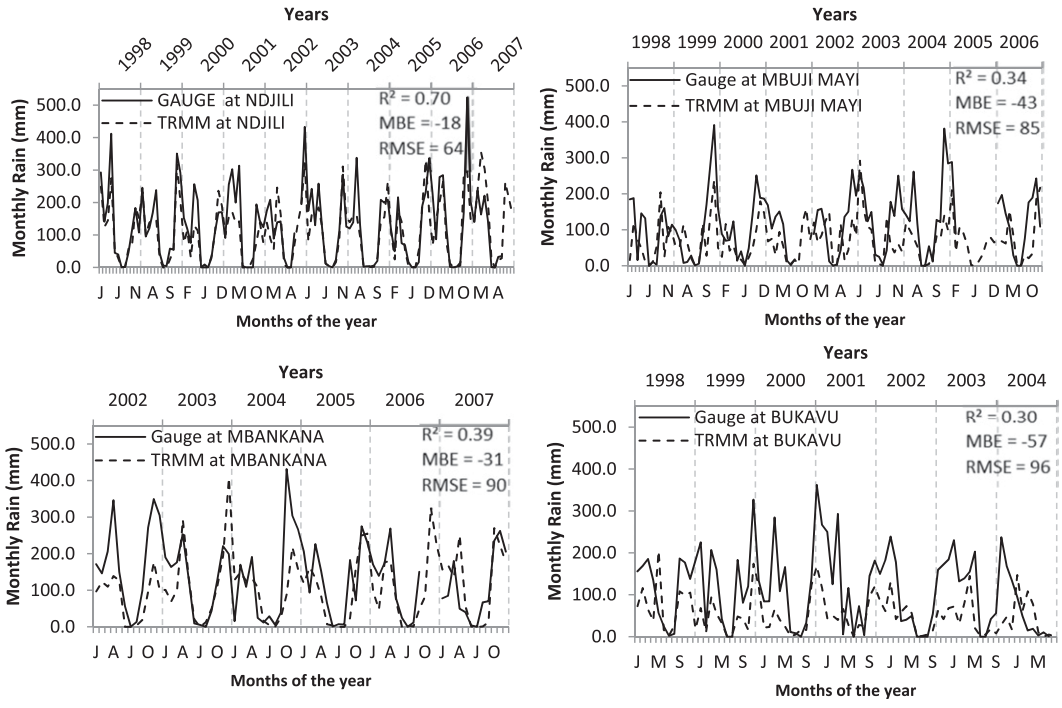

FIG. 3. Version-6 TRMM 3B42 monthly rainfall accumulation (mm) for 10 years (1998–2007) compared with concurrent observed in situ data from gauges. MBE and RMSE are in millimeters.

gauges from the total of 12 used for calibration are shown plotted against concurrent TRMM 3B42 data (Fig. 3). The graphs illustrate the strong seasonal rainfall patterns within the Congo basin. During rainy-season months, an increase in rainfall can be observed, with a corresponding minimum rainfall during dry-season months. The plots of Fig. 3 also show in most cases a tendency toward underestimation of monthly rainfall, most noticeably during the rainy season. The underestimation varies from station to station, with MBE having mostly negative values ranging from −57 to −3 mm. The relatively poor performance exhibited by the product varies from station to station, with low r^2 of the monthly rainfall ranging from 0.15 to 0.70 and relatively high RMSE ranging from 56 to 112 mm.

b. TRMM recalibration

The differences in monthly precipitation totals for the 3B42, 3B43 science product, and recalibrated TRMM data for the entire basin are shown in Fig. 4. When compared with WorldClim climatological data, TRMM 3B42 data underestimate rainfall totals by 12% basin-wide. The 3B43 and recalibrated rainfall estimates add 13% and 15% more precipitation to the total annual rainfall, respectively, relative to TRMM 3B42 estimates. Figure 5 shows the fractional augmentation of precipitation by month of the 3B43 product and the recalibration of this study. All months gain precipitation, with dry-season months (i.e., November–March in the Northern Hemisphere and May–September in the Southern Hemisphere) receiving proportionally greater augmentations. The largest proportional disagreement can be seen in the Southern Hemisphere dry season, where the 3B43 product adds less rainfall proportionally than the recalibration of this study. Results of these datasets are compared with TRMM 3B42 and WorldClim data in Fig. 6. In all products, the seasonal rainfall regime is evident. The position of the basin across the equator subjects the Congo to an alternating seasonal pattern between the Southern and Northern Hemispheres. The passage of the intertropical convergence zone (ITCZ) results in two local rainy and dry seasons of varying length and intensity.

c. Validation

The WorldClim precipitation data of Hijmans et al. (2005) are used as the basis of comparison for validating the recalibrated TRMM data. The recalibrated TRMM data result in uniformly decreasing standard errors of the estimate and root-mean-square errors and corresponding increasing r^2 values (Table 2). Significance tests revealed that all reported correlations are highly significant, with significance level $p < 0.01$ for 30 072 observations. The general improvements validate the regression-tree model in the recalibration of TRMM data. In addition, with values closer to 1, bias measures

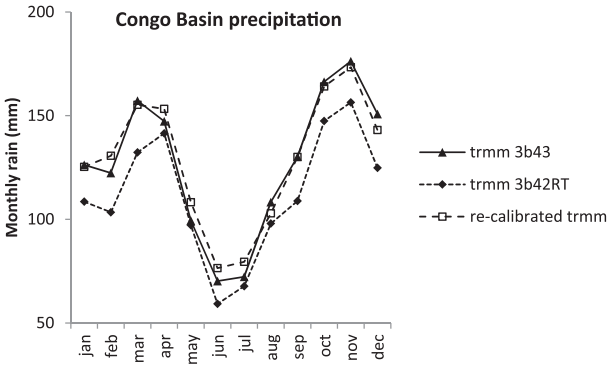

FIG. 4. Rainfall-regime monthly averages for the Congo basin.

show improvements made for every month but July and August, which correspond to the months with lowest rainfall totals for the entire Congo basin (Table 2).

The same comparison was done for the 3B43 and WorldClim precipitation data. Results in Table 2 demonstrate that STEYX of this product is generally greater than the recalibrated TRMM one and is even greater than the TRMM 3B42 in some cases. The recalibrated TRMM r^2 and TRMM 3B43 r^2 are generally similar except in some cases in which the recalibrated TRMM has a stronger correlation with WorldClim precipitation data. Both TRMM 3B43 and recalibrated TRMM have similar biases, with values mostly close to 1 and the 3B43 showing less bias for a majority of the monthly values. MBE values are also generally better using the 3B43 data than using the recalibrated model of this study. Overall, the recalibrated TRMM and TRMM 3B43 are comparable, indicating that the 3B43 extrapolation from the edges of the basin to its interior in the DRC was successfully performed. As well, the sparse data-driven model from limited DRC gauge data performed well in basinwide extrapolation.

d. Climate characterization

Using TRMM 3B43, TRMM 3B42, and recalibrated TRMM precipitation data and WorldClim temperature data grids (Hijmans et al. 2005), digital climate-classification maps for the Congo basin were generated, valid for the 10 years of TRMM that were studied here (1998–2007). With the three TRMM datasets, we quantified a Köppen–Geiger map of seven climate types at a resolution of 0.1° latitude/longitude. The map and the climate-type area totals are shown in Fig. 7 and Table 3, respectively. The most common climate type by land area is tropical savannah (Aw), followed by tropical rain forest (Af), tropical monsoon (Am), humid subtropical (Cwa), temperate (Cwb), highland (H), and hot semiarid (Bsh). For all products, the tropical rain forest climate borders the equator and is surrounded by the tropical monsoon

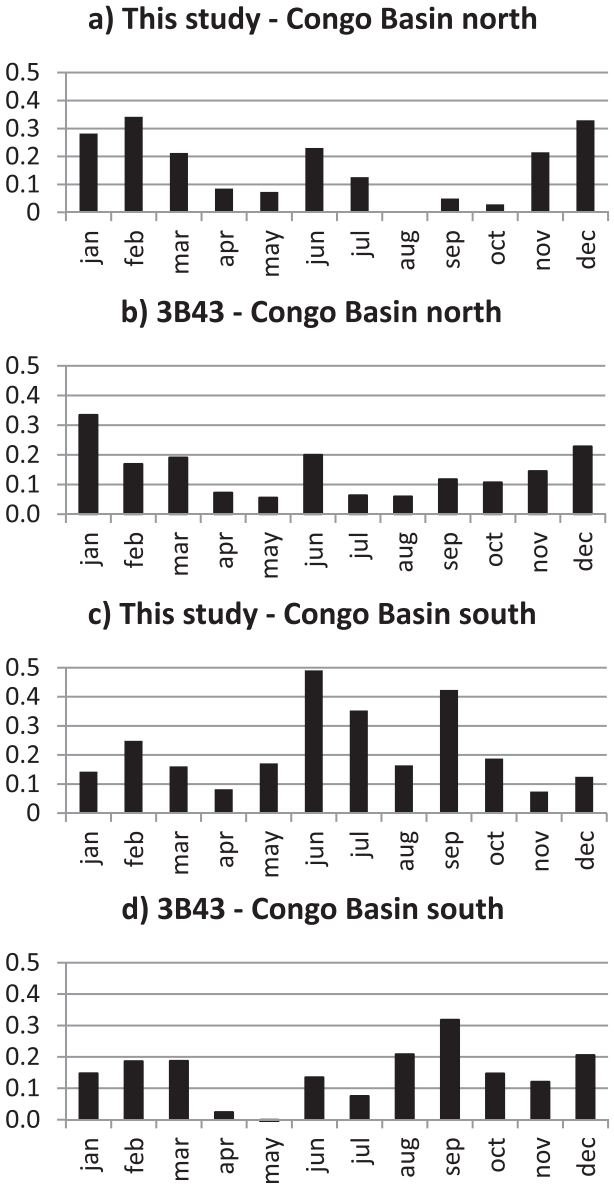

FIG. 5. Monthly fractional augmentation of TRMM 3B42, version 6, average per grid cell for (a) recalibrated TRMM with DRC gauge data and (b) version-7 TRMM 3B43 data for the Congo basin north of the equator. (c),(d) As in (a) and (b), but for the Congo basin south of the equator.

climate, which in turn is surrounded by the tropical savanna climate. The temperate-defined climates are mostly located in the eastern and southeastern highland areas. When using the TRMM 3B42 data to derive a climate classification, a zone of hot semiarid climate (Bsh) in the east and southeast of the basin is erroneously depicted. In addition, the TRMM 3B42 data depict a much narrower band of tropical rain forest and monsoon climate domains. This is indicative of the lower monthly and seasonal rainfall totals of the TRMM 3B42.

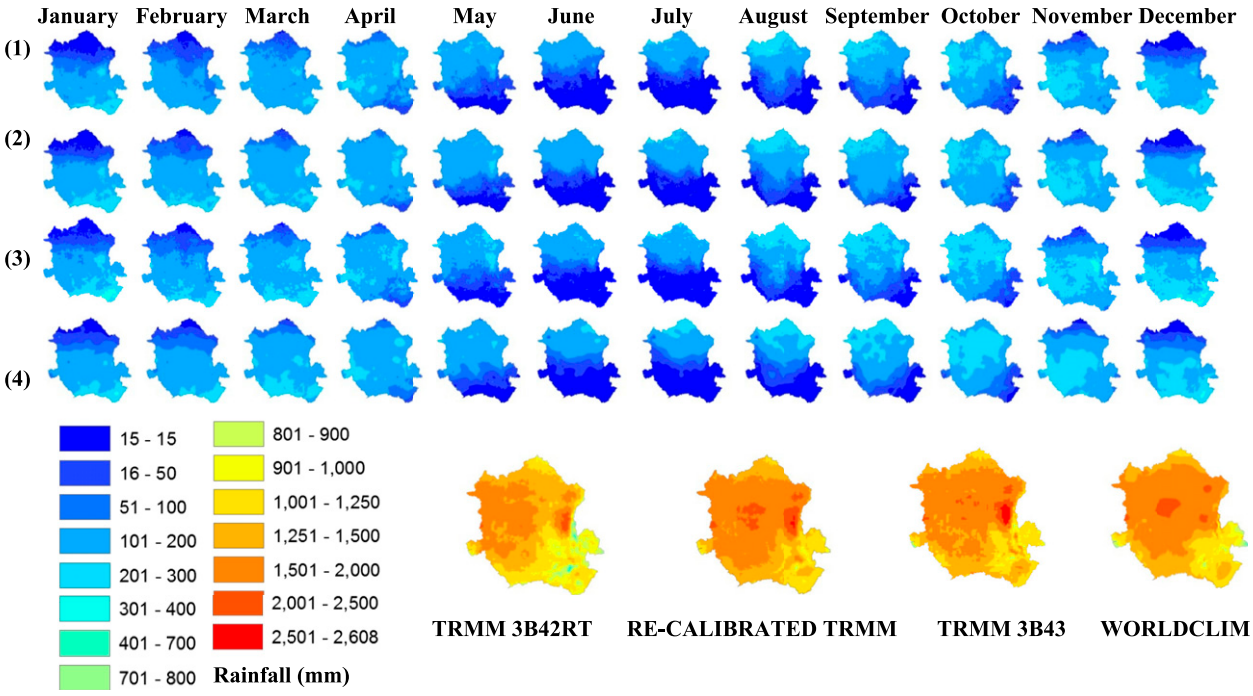

FIG. 6. Mean precipitation for the 12 months of the year and annually; monthly means of version-6 TRMM 3B42 (label 1), recalibrated TRMM (label 2), and version-7 TRMM 3B43 (label 3) are compared with the monthly mean of WorldClim precipitation data (label 4). The 10-yr time series of monthly data from the first three datasets were respectively averaged to depict the basin-scale rainfall regime. The position of the basin across the equator subjects the Congo to an alternate seasonal pattern between the Southern and Northern Hemispheres.

5. Discussion

a. Model performance

Contemporary ground data from rain gauges were used to recalibrate TRMM data, with the resulting modeled precipitation being in agreement with WorldClim data. In general, the model was differentially additive in augmenting monthly TRMM 3B42 data (Fig. 5). The 75th-percentile and the 90th-percentile monthly TRMM metrics derived from the daily 3B42 data were the most significant variables among all inputs in predicting gauge-measured monthly rainfall totals. These two variables accounted for 44% and 19% of the reduction of overall sum of squares, respectively. The first split in the bagged trees employed the 75th percentile 16 times with a mean threshold of 1.2 mm of precipitation. Less than this value resulted in an average child node of 30 mm of monthly precipitation; greater than this gave the average estimated monthly precipitation as 172 mm. Another six trees employed the 90th percentile with a mean threshold of 3.7 mm of precipitation and child nodes of 25 and 176 mm of precipitation. Subsequent splits further refined the estimates beyond these initial thresholds. In general, if 10%–25% of the daily rainfall per month was greater than 1.2–3.7 mm, that month had mean gauge-measured precipitation of greater than 170 mm. If the frequency of such rains was less than this range, the mean gauge-measured precipitation was less than 30 mm. After these two percentile metrics came the monthly 3B42 totals, which explained 12% of the model's reduction in sum of squares. Results illustrate the value of statistical derivatives of the daily data in predicting monthly precipitation. The generalized bagged regression-tree model does not fit well to outliers, however, and there was no sensitivity to monthly rainfall greater than 300 mm. This result could be due to the limited number of high monthly input observations coupled with a lack of separability of these months in the statistical feature space.

The general deficit observed by the TRMM 3B42 inputs could be explained by omitted rainfall events, specifically a lack of sensitivity to different types of rain by TRMM sensors. TRMM 3B42 data are known to omit rainy-season convective storms, leading to possible rainy-season underestimation of precipitation. TRMM 3B42 data are also insensitive to light-rain events; such light-rain events, which are characteristic of stratiform rain in the region, are more frequent during the Congo basin dry season. These two sources of rain-event omission (missing rainy-season convective and missing dry-season stratiform rain events) could explain the general underestimation of rainfall throughout the year.

TABLE 2. Basinwide STEYX, r^2 and bias, MBE (mm), and RMSE (mm) for TRMM 3B42 (label o), recalibrated TRMM (label r), and TRMM 3B43 (label 3b) in comparison with WorldClim monthly precipitation totals. The best performing products per statistical measure are shown in boldface type.

	STEYX (o)	STEYX (r)	STEYX (3b)	r^2 (o)	r^2 (r)	r^2 (3b)	Bias (o)	Bias (r)	Bias (3b)	MBE (o)	MBE (r)	MBE (3b)	RMSE (o)	RMSE (r)	RMSE (3b)
Jan	28	**25**	30	0.85	**0.89**	0.88	0.86	0.99	**1.00**	−18.06	−1.30	**−0.31**	33.86	**24.87**	30.25
Feb	27	**24**	25	0.73	**0.84**	**0.84**	0.83	1.05	**0.99**	−20.57	6.70	**−1.61**	36.57	24.69	**24.67**
Mar	27	**22**	29	0.63	**0.74**	0.72	0.79	0.93	**0.94**	−35.08	−12.13	**−10.15**	45.75	**26.85**	30.83
Apr	30	**21**	29	0.63	**0.71**	0.66	0.90	**0.98**	0.94	−15.11	**−3.31**	−9.29	34.18	**24.12**	30.83
May	24	**20**	28	0.86	**0.91**	0.84	0.91	**1.01**	0.93	−9.82	**1.26**	−7.60	27.25	**20.72**	28.90
Jun	**18**	**18**	**18**	0.91	0.93	**0.94**	0.85	1.10	**1.01**	−10.19	7.03	**0.78**	25.94	19.71	**17.84**
Jul	24	**20**	**20**	0.89	**0.93**	**0.93**	0.97	1.14	**1.03**	**−2.04**	9.68	2.44	25.57	22.57	**20.91**
Aug	31	**22**	27	0.87	**0.92**	0.91	**1.04**	1.09	1.15	**3.76**	8.72	14.07	31.93	**25.28**	30.52
Sep	25	**19**	25	0.89	**0.93**	0.91	0.85	**1.02**	**1.02**	−18.73	**2.52**	2.60	32.59	**23.21**	25.02
Oct	28	**20**	28	0.84	**0.87**	0.85	0.90	**0.99**	**1.01**	−17.07	**−0.44**	1.85	33.32	**26.77**	28.18
Nov	32	**22**	33	0.74	**0.81**	0.74	0.92	**1.02**	1.04	−12.89	**4.08**	6.93	34.86	**25.86**	34.05
Dec	34	**26**	29	0.79	**0.89**	**0.89**	0.83	0.96	**1.00**	−24.79	−6.51	**1.20**	44.01	**27.45**	29.86
Annual	188	**143**	199	0.58	**0.70**	0.54	0.88	1.01	**1.00**	−177.78	20.75	**5.34**	268.30	**162.37**	212.07

b. *Climate classification*

Both the 3B43 and recalibrated TRMM-derived climate maps compare favorably to the updated world map of the Köppen–Geiger climate classification of Peel et al. (2007) (Fig. 7 and Table 3). The temperate and humid subtropical climates are significantly more represented in Peel's map, however. Peel et al. (2007, p. 1638) explained a source of uncertainty for these two classes by reporting, "The low density of temperature stations in Africa resulted in some climate types extending further than expected, which could not be corrected due to lack of data. The two regions where this is most evident are the temperate regions in the Eastern Rift Valley south of Nairobi, Kenya and around Antananarivo, Madagascar. In both of these cases the temperature stations are in high elevation locations (Nairobi and Antananarivo) and experience a temperate climate type. However, due to the lack of nearby lower elevation temperature stations, the temperate influence of both these high elevation stations extends well beyond their immediate location and large regions of temperate climate type result in regions that are more likely to be tropical." The WorldClim temperature data used for this study have the slight advantage of having fewer spatial data gaps than do the temperature data used by Peel et al. (2007), resulting in a reduced extent of continental climate types (Cwb and Cwa) for all TRMM-derived climate maps (Fig. 7).

Table 3 compares the different areas of climate classes among the four products. Class membership as a percentage of the overall study area varied greatly. At 72%, 65%, 66%, and 52% of the TRMM 3B42-derived climate map, recalibrated TRMM-derived climate map, TRMM 3B43-derived climate map, and Peel's climate map, respectively, the tropical wet and dry climate class (Aw) is by far the most abundant in the Congo basin. The tropical rain forest class (Af) is the next most plentiful at 10%, 17%, 16%, and 15% of the four respective maps. In the TRMM 3B42-derived climate map, the tropical monsoon class (Am) extent is equal to that of tropical rain forest.

The derived climate maps from 3B43 and from the recalibrated product of this study have high agreement (91%). Overall agreement with Peel et al. was 63% when employing the climate classification with TRMM 3B42 inputs. Agreement rose to 69% and 70% when using TRMM 3B43 and the recalibrated TRMM inputs, respectively. The tropical rain forest class (Af) agreement increased by 70%, and the tropical monsoon (Am) class agreement increased by 111% for the recalibrated product. While Peel's map cannot be taken as truth, the intercomparison points out some strengths of the TRMM-derived climate map using the gauge-calibrated results of the present study. First, the tropical rain forest and monsoon climates are more accurately depicted. Second, the hot semiarid climate and the hot desert climate are not characterized at all. Third, the highland climate is captured. The overall performance of the recalibrated TRMM-derived climate classifier is promising, although its application in other regions would most likely require local TRMM recalibration with appropriate ground data.

c. *Application of recalibrated TRMM in characterizing seasonal rainfall*

Waliser and Gauthier (1993) quantified the annual cycle of ITCZ migration and its occurrence in the African continent. As described by McGregor and Nieuwolt (1998), a zone of maximum rainfall related to the African ITCZ follows the solar declination with a delay of about 1 month. The ITCZ passes through the Southern Hemisphere from October to April and the Northern Hemisphere from

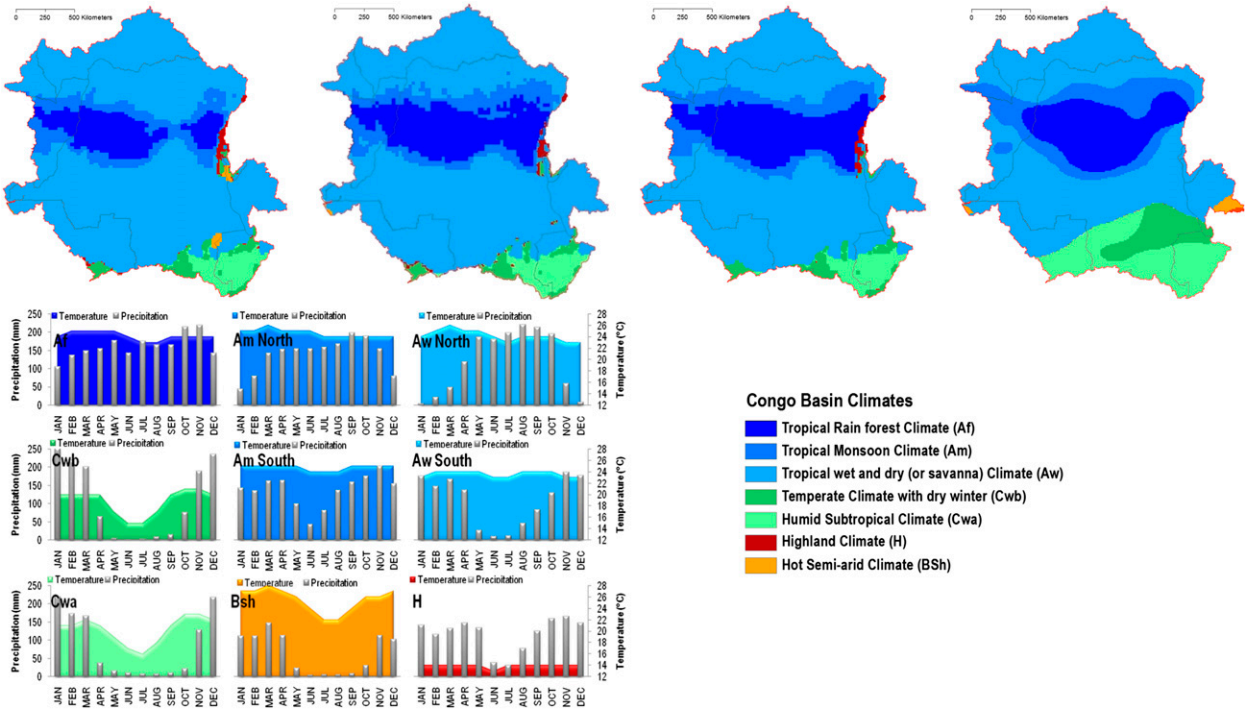

FIG. 7. The K–G climate classifications for the Congo basin on the basis of (left) version-6 TRMM 3B42, (center left) version-7 TRMM 3B43, and (center right) recalibrated TRMM precipitation data, all with WorldClim temperature data. Also shown are (right) those of Peel et al. (2007). The graphs illustrate the recalibrated TRMM monthly-mean precipitation and WorldClim monthly-mean temperature for representative sites in the recalibrated TRMM-derived climate map.

April to October. Our results show April and October to be the peak rainfall months for both hemispheres. This is consistent with Waliser and Gauthier's model that places the ITCZ position near the equator during these two months. Suzuki (2011) explained the driving forces of the seasonal variation of the ITCZ and found that the origin of the water vapor fluxes feeding the ITCZ varied by season. In April, the water vapor flux is mostly derived from the Indian Ocean via Tanzania. In October, the water vapor flux is supplied from within the Congo basin. Varying sources of water vapor could explain the difference between the two peak rainfall months (April and October) observed across the basin.

The bimodal pattern of precipitation in the Congo basin is illustrated in Fig. 4. The larger rainy season occurs after the autumnal equinox, as the ITCZ returns from the north and crosses the Congo basin. The peak basinwide rainfall total of November reflects this. The return of the ITCZ from the south does not result in a similar magnitude of rainfall. This intra-annual variation in Congo basin rainfall is present in all products. Given this fact, we now examine seasonality using the recalibrated TRMM data of this study. Figure 8a shows the month of maximum rainfall and the fact that the ITCZ migration from north to south from August through January represents the peak precipitation totals across the basin. There is a bimodal seasonality, but it is not "mirrored" or proportional between the two rainy-season peaks.

All areas of the basin likewise experience two dry seasons. The farther from the equator one looks, the more different the dry seasons are in terms of length and precipitation totals. As the ITCZ heads south or north it leaves the Congo basin, and for all regions of the basin a dry season occurs. For regions on the same side of the equator as the ITCZ during a solstice, this period is often referred to as the "little" dry season. The period during which the ITCZ is at its farthest distance from any locality falls within the time of the local "big" dry season. Figure 8b shows the ratio of the big dry season's minimum rainfall to the little dry season's minimum rainfall. The actual equator is very close to this "precipitation" equator, because only a very small band of area near/south of the actual equator features balanced dry-season minima.

The white brackets in Fig. 8b delimit a north–south transect that is displayed graphically in Fig. 9. The plot depicts the set of mean monthly precipitation values for 1° squares from 0° to 8° north and south, along a transect from 22° to 23° east in the middle of the basin. After equinoxes, there is high rainfall across all latitudes within the basin. Before equinoxes, there is a wider range of precipitation across all latitudes within the basin. This plot is a sample across latitudes and confirms that, per

TABLE 3. Classification results by area (km^2 divided by 1000) and as a percentage of total Congo basin area (3 700 000 km^2). Given are climate-class totals of climate maps derived from TRMM 3B42, recalibrated TRMM, and TRMM 3B43 products and the map of Peel et al. (2007).

Climate class	TRMM 3B42–derived climate map	Recalibrated TRMM–derived climate map	TRMM 3B43–derived climate map	Peel's climate map
Tropical rain forest (Af)	369 (10%)	627 (17%)	574 (16%)	559 (15%)
Tropical monsoon (Am)	361 (10%)	403 (11%)	406 (11%)	474 (13%)
Tropical wet and dry (Aw)	2689 (72%)	2393 (65%)	2447 (66%)	1932 (52%)
Temperate (Cwb)	109 (3%)	108 (3%)	98 (3%)	227 (6%)
Humid subtropical (Cwa)	153 (4%)	148 (4%)	151 (4%)	482 (13%)
Highland (H)	28 (1%)	21 (1%)	25 (1%)	0

unit area, the Congo basin receives more rain in the August–December time frame than in the mirrored period of the year of February–June. Again, the southward movement of the ITCZ is the dominant rain mechanism over the basin.

If one assumes a conceptual model in which there is no difference in the rainfall amounts associated with the twice-yearly passing of the ITCZ and there are equal areas of catchment north and south of the equator, mirrored or symmetrical intra-annual precipitation would be expected on each side of the equator. This is clearly not the case, and the asymmetry is due to two principal factors. First, the basin extends nearly 2 times as far to the south of the equator as to the north; the southern portion accounts for two-thirds of the overall catchment area. The ITCZ's proportionally greater presence in the south leads to a corresponding proportional increase in rainfall associated with the periods of ITCZ passage. Another cause is the greater rainfall associated with the southern movement of the ITCZ than with its northern movement, as documented in the preceding discussion. Suzuki (2011) identified seasonally varying water vapor fluxes for the ITCZ. The post-autumnal-equinox source of the Congo basin itself leads to greater precipitation than the post-vernal-equinox source of the Indian Ocean. The deviation from the symmetrical model can be seen as well in the stream hydrograph at Kinshasa, the capital of the DRC. The Kinshasa gauge station is situated along the lower reaches of the Congo River, roughly 400 km from the ocean. The area upstream from the gauge station (the "area to point" watershed) encompasses more than 90% of the Congo basin watershed. Figure 10 shows two peaks of high streamflow, with one in the November timeframe constituting a clear maximum annual flow. The secondary peak is in April, the expected symmetrical counterpart. The streamflow of April is roughly 50%–80% of the

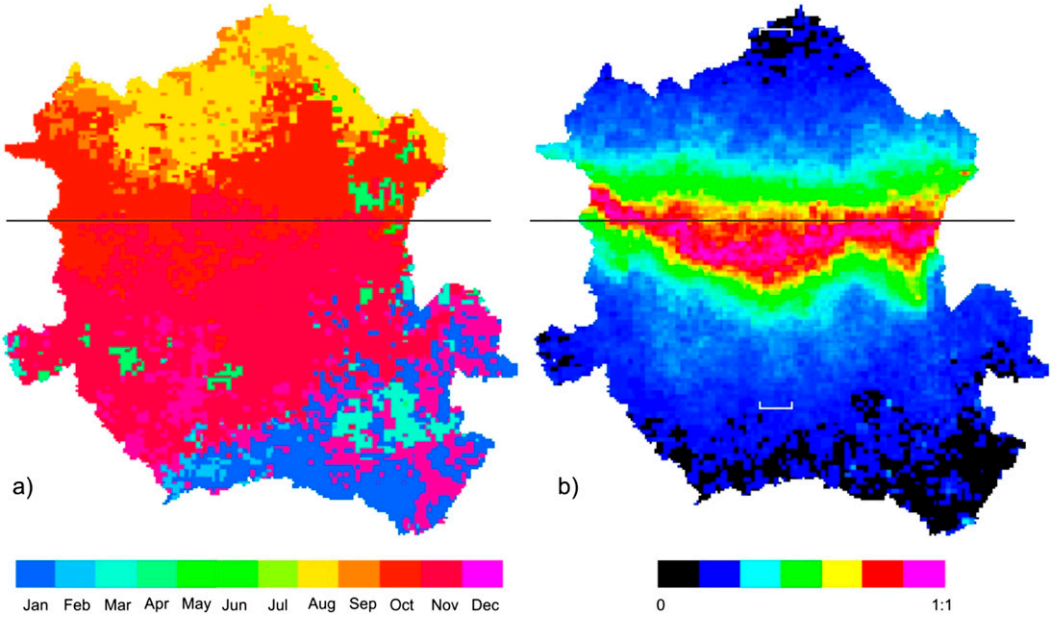

FIG. 8. (a) Month of maximum precipitation for recalibrated TRMM data. (b) Ratio of big to small dry-season precipitation minima.

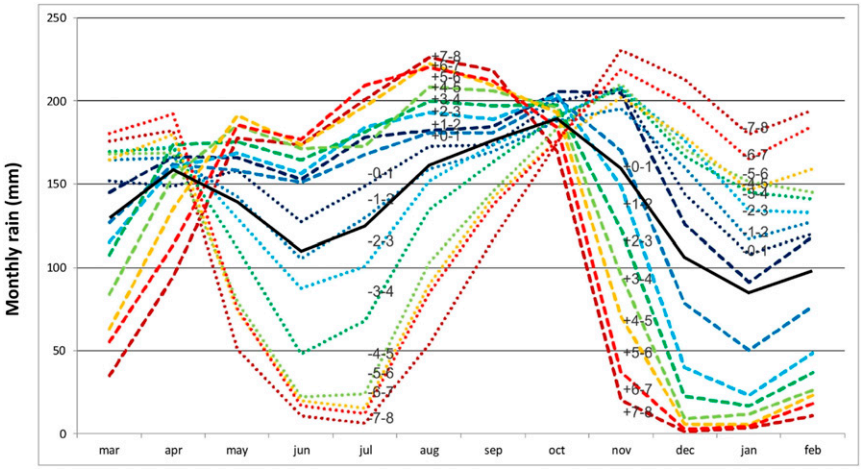

FIG. 9. Plots of monthly precipitation for 1° blocks from +8° to −8° latitude for the transect along 22°–23°E longitude (brackets in Fig. 8b show the area). Dashed and dotted lines are latitudes north and south of the equator, respectively. Colors correspond to latitudinal increments of 1° and are labeled. The black line is the transect monthly means.

November streamflow, however. In testing the three monthly TRMM precipitation products against the stream gauge data of Kinshasa, including time lags, the highest correlation of 0.81 was found for the recalibrated TRMM model with a 1-month lag (Fig. 10).

6. Conclusions

This study indicates that version-6 TRMM 3B42 data are appropriate for quantifying Congo basin rainfall regimes and for deriving climate maps when calibrated by ground gauge datasets from within the region. Two products—version 7 of the TRMM 3B43, calibrated by ground data located largely at the periphery of the Congo basin, and a new product, calibrated using ground data within the central Congo basin—yielded viable precipitation and climate characterizations. Despite having no ground calibration sites within the DRC, the version-7 TRMM 3B43 product accurately depicted Congo basin precipitation without bias. The sparse-data model employed in this study also compared well to ancillary data. The generalized statistical feature space derived from daily accumulations of version-6 TRMM 3B42 observations enabled the extrapolation of monthly recalibrated rainfall from only 12 gauge stations. Recalibration of TRMM data resulted in a general augmentation of rainfall for both local rainy and dry seasons and a slight bias relative to the version-7 TRMM 3B43 science product. Although the new model was insensitive to high-precipitation events, the general depiction at mean annual and monthly time scales also agreed well with WorldClim data, although exhibiting a slight bias. Added rainfall was absolutely higher during rainy-season months and relatively higher during dry-season months. These results indicate that both warm, convective-driven and cool, stratiform-driven rain regimes were underestimated by the version-6 TRMM 3B42 estimates. All products were consistent in the depiction of intra-annual variation (Fig. 4); the dominance of post-autumnal-equinox rainfall was captured in observed downstream Congo River hydrographs, pointing the way forward for more substantive modeling of streamflow using TRMM, either the standard 3B43 or new products such as the one presented here. Climate characterizations using the version-7 3B43 and recalibrated results of this study resulted in nearly equal areas for the climate types found within the Congo basin. The study serves as a demonstration of an alternative approach to processing TRMM data in characterizing regional precipitation regimes as well as a validation of

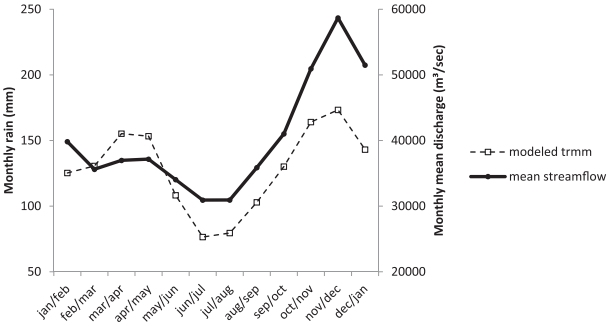

FIG. 10. Recalibrated/modeled TRMM Congo basin monthly precipitation and Congo River mean streamflow discharge at Kinshasa from 2000 to 2007 (data are from the DRC waterway public company Régie des voies fluviales). Congo River streamflow is offset by 1 month from the precipitation data (e.g., label jan/feb represents January rainfall and February streamflow at Kinshasa.

the version-7 TRMM 3B43 science product for a poorly covered region of Africa.

Acknowledgments. This study was made possible through funding provided by the NASA Earth and Space Science Fellowship (Grant NNX09AN99H) and by the U.S. Agency for International Development through its Central Africa Regional Program for the Environment (CARPE). The authors are very grateful to the TRMM Science Team at NASA/GSFC, who are responsible for the development of the TRMM Multisatellite Precipitation Analysis algorithm, and to the Precipitation Processing System (PPS) science team who computed the TRMM science product used in this study "TRMM and Other Data Precipitation Data Set" 3B43, version 7, as well as the version-6 TRMM 3B42 science product. The authors are also grateful to USGS/EROS, which performed post-processing and distribution of the value-added daily datasets accumulated from NASA TRMM 3B42 and used in this study. The authors thank the Democratic Republic of the Congo meteorological agency Agence Nationale de Météorologie et de Télédétection par Satellite (METTELSAT) and the Democratic Republic of the Congo waterway public company Régie des voies fluviales (RVF) for sharing their ground information.

REFERENCES

Adeyewa, Z. D., and K. Nakamura, 2003: Validation of TRMM radar rainfall data over major climatic regions in Africa. *J. Appl. Meteor. Climatol.,* **42,** 331–347, doi:10.1175/1520-0450(2003)042<0331:VOTRRD>2.0.CO;2.

Bitew, M. M., and M. Gebremichael, 2011: Are satellite-gauge rainfall products better than satellite-only products for Nile hydrology? *Nile River Basin,* A. M. Melesse, Ed., Springer-Verlag, 129–141.

Breiman, L., 1996: Bagging predictors. *Mach. Learn.,* **24,** 123–140.

——, J. H. Friedman, R. A. Olsen, and C. J. Stone, 1984: *Classification and Regression Trees.* Wadsworth Statistics and Probability Series, Taylor and Francis, 368 pp.

Dinku, T., P. Ceccato, E. Grover-Kopec, M. Lemma, S. J. Connor, and C. F. Ropelewski, 2007: Validation of satellite rainfall products over East Africa's complex topography. *Int. J. Remote Sens.,* **28,** 1503–1524, doi:10.1080/01431160600954688.

——, S. Chidzambwa, P. Ceccato, S. J. Connor, and C. F. Ropelewski, 2008: Validation of high-resolution satellite rainfall products over complex terrain. *Int. J. Remote Sens.,* **29,** 4097–4110, doi:10.1080/01431160701772526.

——, S. J. Connor, and P. Ceccato, 2010: Comparison of CMORPH and TRMM-3B42 over mountainous regions of Africa and South America. *Satellite Rainfall Applications for Surface Hydrology,* M. Gebremichael and F. Hossain, Eds., Springer-Verlag, 193–204.

Ebert, E. E., J. E. Janowiak, and C. Kidd, 2007: Comparison of near-real-time precipitation estimates from satellite observations and numerical models. *Bull. Amer. Meteor. Soc.,* **88,** 47–64, doi:10.1175/BAMS-88-1-47.

Gabella, M., S. Michaelides, P. Constantinides, and G. Perona, 2006: Climatological validation of TRMM Precipitation Radar monthly rain products over Cyprus during the first 5 years (December 1997 to November 2002). *Meteor. Z.,* **15,** 559–564, doi:10.1127/0941-2948/2006/0158.

——, S. Athanasatos, R. Notarpietro, and S. Michaelides, 2008: Climatological validation of TRMM radar monthly rainfall amounts over Cyprus during the first 8 years (December 1997–November 2005). *Fifth European Conf. on Radar in Meteorology and Hydrology*, Helsinki, Finland, ERAD, 5 pp. [Available online at http://www.erad2010.org/pdf/POSTER/Wednesday/03_Satellite/03_ERAD2010_0023_extended.pdf.]

Herrmann, S., and K. A. Mohr, 2011: A continental-scale classification of rainfall seasonality regimes in Africa based on gridded precipitation and land surface temperature products. *J. Appl. Meteor. Climatol.,* **50,** 2504–2513, doi:10.1175/JAMC-D-11-024.1.

Hijmans, R. J., S. E. Cameron, J. L. Parra, P. Jones, and A. Jarvis, 2005: Very high resolution interpolated climate surfaces for global land areas. *Int. J. Climatol.,* **25,** 1965–1978, doi:10.1002/joc.1276.

Houze, R. A., Jr., 1997: Stratiform precipitation in regions of convection: A meteorological paradox? *Bull. Amer. Meteor. Soc.,* **78,** 2179–2196, doi:10.1175/1520-0477(1997)078<2179:SPIROC>2.0.CO;2.

Huffman, G. J., 2013: README for accessing experimental real-time TRMM Multi-Satellite Precipitation Analysis (TMPA-RT) data sets. NASA Goddard Space Flight Center Mesoscale Atmospheric Processes Laboratory Rep., 11 pp. [Available online at ftp://meso-a.gsfc.nasa.gov/pub/trmmdocs/rt/3B4XRT_README.pdf.]

——, and D. T. Bolvin, 2014: TRMM and other data precipitation data set documentation: "Recent" news. NASA Goddard Space Flight Center Mesoscale Atmospheric Processes Laboratory Rep., 42 pp. [Available online at ftp://precip.gsfc.nasa.gov/pub/trmmdocs/3B42_3B43_doc.pdf.]

——, and Coauthors, 1997: The Global Precipitation Climatology Project (GPCP) combined precipitation dataset. *Bull. Amer. Meteor. Soc.,* **78,** 5–20, doi:10.1175/1520-0477(1997)078<0005:TGPCPG>2.0.CO;2.

——, R. F. Adler, D. T. Bolvin, G. Gu, E. J. Nelkin, K. P. Bowman, E. F. Stocker, and D. B. Wolff, 2007: The TRMM Multi-satellite Precipitation Analysis (TMPA): Quasi-global, multiyear, combined-sensor precipitation estimates at fine scales. *J. Hydrometeor.,* **8,** 38–55, doi:10.1175/JHM560.1.

——, ——, ——, and E. J. Nelkin, 2010: The TRMM Multi-satellite Precipitation Analysis (TMPA). *Satellite Rainfall Applications for Surface Hydrology,* F. Hossain and M. Gebremichael, Eds., Springer-Verlag, 3–22.

Köppen, W., 1884: Die Wärmezonen der Erde, nach der Dauer der heissen, gemässigten und kalten Zeit und nach der Wirkung der Wärme auf die organische Welt betrachtet (The thermal zones of the earth according to the duration of hot, moderate and cold periods and to the impact of heat on the organic world). *Meteor. Z.,* **1,** 215–226; E. Volken and S. Brönnimann, Trans. and Eds., 2011: *Meteor. Z.,* **20,** 351–360, doi:10.1127/0941-2948/2011/105.

——, 1918: Klassification der Klimate nach Temperatur, Niederschlag und Jahreslauf (Classification of climates according to temperature, precipitation and seasonal cycle). *Petermanns Geogr. Mitt.,* **64,** 193–203, 243–248. [Available online at http://koeppen-geiger.vu-wien.ac.at/pdf/Koppen_1918.pdf.]

Kottek, M., J. Grieser, C. Beck, B. Rudolf, and F. Rubel, 2006: World map of the Köppen–Geiger climate classification updated. *Meteor. Z.,* **15,** 259–263, doi:10.1127/0941-2948/2006/0130.

McGregor, G. R., and S. Nieuwolt, 1998: *Tropical Climatology.* 2nd ed. John Wiley and Sons, 339 pp.

Nicholson, S. E., 2000: The nature of rainfall variability over Africa on time scales of decades to millennia. *Global Planet. Change,* **26,** 137–158, doi:10.1016/S0921-8181(00)00040-0.

——, and Coauthors, 2003: Validation of TRMM and other rainfall estimates with a high-density gauge dataset for West Africa. Part II: Validation of TRMM rainfall products. *J. Appl. Meteor. Climatol.,* **42,** 1355–1368, doi:10.1175/1520-0450(2003)042<1355:VOTAOR>2.0.CO;2.

Peel, M. C., B. L. Finlayson, and T. A. McMahon, 2007: Updated world map of the Köppen–Geiger climate classification. *Hydrol. Earth Syst. Sci.,* **11,** 1633–1644, doi:10.5194/hess-11-1633-2007.

Roca, R., P. Chambon, I. Jobard, P. E. Kirstetter, M. Gosset, and J. C. Berges, 2010: Comparing satellite and surface rainfall products over West Africa at meteorologically relevant scales during the AMMA campaign using errors estimates. *J. Appl. Meteor. Climatol.,* **49,** 715–731, doi:10.1175/2009JAMC2318.1.

Rudolf, B., 1993: Management and analysis of precipitation data on a routine basis. *Proc. Int. WMO/IAHS/ETH Symp. on Precipitation and Evaporation,* Bratislava, Slovakia, Slovak Hydrometeorology Institute, 69–76.

——, H. Hauschild, W. Ruth, and U. Schneider, 1994: Terrestrial precipitation analysis: Operational method and required density of point measurements. *Global Precipitations and Climate Change,* M. Dubois and F. Desalmand, Eds., Springer-Verlag, 173–186.

Schumacher, C., and R. A. Houze Jr., 2003: Stratiform rain in the tropics as seen by the TRMM Precipitation Radar. *J. Climate,* **16,** 1739–1756, doi:10.1175/1520-0442(2003)016<1739:SRITTA>2.0.CO;2.

Suzuki, T., 2011: Seasonal variation of the ITCZ and its characteristics over central Africa. *Theor. Appl. Climatol.,* **103,** 39–60, doi:10.1007/s00704-010-0276-9.

Tierney, J. E., J. M. Russell, J. S. Sinninghe Damsté, Y. Huang, and D. Verschuren, 2011: Late Quaternary behavior of the East African monsoon and the importance of the Congo air boundary. *Quat. Sci. Rev.,* **30,** 798–807, doi:10.1016/j.quascirev.2011.01.017.

Waliser, D. E., and C. Gauthier, 1993: A satellite-derived climatology of the ITCZ. *J. Climate,* **6,** 2162–2174, doi:10.1175/1520-0442(1993)006<2162:ASDCOT>2.0.CO;2.

Zhou, L., and Coauthors, 2014: Widespread decline of Congo rainforest greenness in the past decade. *Nature,* **509,** 86–90, doi:10.1038/nature13265.